Conference Paper, Published Version

Matsumoto, Junichi

Orthogonal Basis Bubble Function Finite Element Method for Shallow Water Equations

ORTHOGONAL BASIS BUBBLE FUNCTION FINITE ELEMENT METHOD FOR SHALLOW WATER EQUATIONS

Junichi Matsumoto[1]

[1] Research Scientist, Advanced Manufacturing Research Institute (AMRI),
National Institute of Advanced Industrial Science and Technology (AIST),
1-2-1 Namiki,Tsukuba, Ibaraki 305-8564, Japan, e-mail: junmcct@ni.aist.go.jp

ABSTRACT

In this paper, an orthogonal basis bubble function element stabilization method for shallow water long wave equation is proposed. The result of the diagonal mass matrix using the orthogonal basis bubble function element is in a better agreement with a exact solution than the result of the lumped mass matrix using the linear bubble function element. The bubble function method stabilization method obtained better numerical accuracy and stability than the classical bubble function method with Bubnov-Galerkin formulation.

Keywords: shallow water equation, orthogonal basis bubble function element stabilization method, finite element method

1. INTRODUCTION

Recently, it was found that bubble function element in finite element method based on Bubnov-Galerkin formulation operate a stabilizing role in certain kind of problem (Pierre, 1988; Baicocchi *et al.*, 1993). For steady advection diffusion problem, the Bubnov-Galerkin method employing the piecewise linear interpolation with bubble function is equivalent to the streamline-upwind/Petrov-Galerkin (SUPG) finite element method (Brooks and Hughes, 1982) using P1 approximation. In this framework, some researchers have developed the advanced bubble function elements for the advection diffusion problem (Simo *et al.*, 1995; Yamada, 1998). The advanced bubble function elements are established by using the bubble function with a scaling parameter according to the cell Peclet number to attain optimal numerical diffusion. Authors (Matsumoto *et al.*, 2003) have applied this approach to shallow water long wave problem by using special bubble functions with two-level three-level partitions. The special bubble functions with two-level three-level partitions are extended as orthogonal basis bubble function element stabilization method for P1B element (Matsumoto, 2005). An important point to be noted is that the consistent mass matrix is a diagonal matrix on account of the orthogonal intersection of the basis functions of the orthogonal basis bubble function element. Therefore, an explicit finite element method with orthogonal basis bubble function element is proposed in this paper. The orthogonal basis bubble function element stabilization method obtains better stability than the classical bubble function element method.

2. BASIC EQUATION

The shallow water long wave equation to the coordinate system of Figure 1 is written as the following momentum equation and continuity equation.

$$\dot{\boldsymbol{u}} + \boldsymbol{\mathcal{L}}(\boldsymbol{u})\boldsymbol{u} + \boldsymbol{N}(\boldsymbol{u})\boldsymbol{u} = \boldsymbol{f} \quad in \quad \Omega \times [0, T]. \tag{1}$$

Here,

$$\boldsymbol{\mathcal{L}}(\boldsymbol{u}) := \sum_{i=1}^{2} \left\{ \boldsymbol{A}(\boldsymbol{u})_i \frac{\partial}{\partial x_i} - \sum_{j=1}^{2} \frac{\partial}{\partial x_i} \left(\boldsymbol{\nu}_{ij} \frac{\partial}{\partial x_j} \right) \right\} = \boldsymbol{A}(\boldsymbol{u})_i \frac{\partial}{\partial x_i} - \frac{\partial}{\partial x_i} \left(\boldsymbol{\nu}_{ij} \frac{\partial}{\partial x_j} \right) ,$$

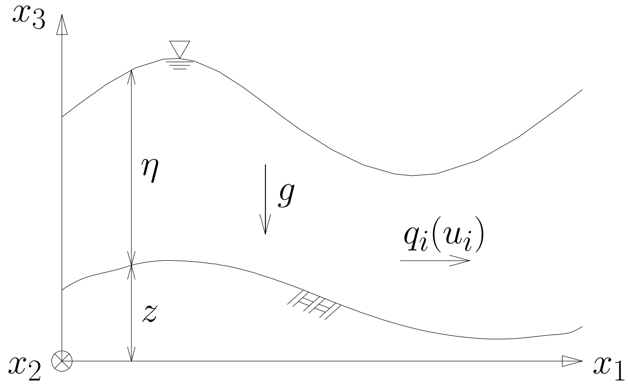

Figure 1: Coordinate system.

$$\boldsymbol{A}(\boldsymbol{u})_1 = \begin{bmatrix} 0 & 1 & 0 \\ c^2 - u_1^2 & 2u_1 & 0 \\ -u_1 u_2 & u_2 & u_1 \end{bmatrix} , \ \boldsymbol{A}(\boldsymbol{u})_2 = \begin{bmatrix} 0 & 0 & 1 \\ -u_1 u_2 & u_2 & u_1 \\ c^2 - u_2^2 & 0 & 2u_2 \end{bmatrix} ,$$

$$\boldsymbol{\nu}_{11} = (\nu_e + \delta) \begin{bmatrix} \nu_\eta & 0 & 0 \\ -2u_1 & 2 & 0 \\ -u_2 & 0 & 1 \end{bmatrix} , \ \boldsymbol{\nu}_{12} = (\nu_e + \delta) \begin{bmatrix} 0 & 0 & 0 \\ 0 & 0 & 0 \\ -u_1 & 1 & 0 \end{bmatrix} ,$$

$$\boldsymbol{\nu}_{21} = (\nu_e + \delta) \begin{bmatrix} 0 & 0 & 0 \\ -u_2 & 0 & 1 \\ 0 & 0 & 0 \end{bmatrix} , \ \boldsymbol{\nu}_{22} = (\nu_e + \delta) \begin{bmatrix} \nu_\eta & 0 & 0 \\ -u_1 & 1 & 0 \\ -2u_2 & 0 & 2 \end{bmatrix} ,$$

$$\boldsymbol{N}(\boldsymbol{u}) = \begin{bmatrix} 0 & 0 & 0 \\ 0 & \frac{u_*}{\eta} - f & 0 \\ 0 & 0 & \frac{u_*}{\eta} + f \end{bmatrix} , \ \boldsymbol{f} = \begin{bmatrix} 0 \\ -c^2 z_{,1} + f_1 \\ -c^2 z_{,2} + f_2 \end{bmatrix} ,$$

$$u_* = \frac{g n^2 \sqrt{u_1^2 + u_2^2}}{\eta^{1/3}} , \ \nu_e = \frac{k}{6} u_* \eta , \ f = 2\omega \sin\phi , \ f_i = \frac{\rho_a}{\rho} c_s \sqrt{w_1^2 + w_2^2} \, w_i , \ \boldsymbol{u} = [\eta, q_1, q_2]^T .$$

η and q_i are the water depth and discharge of unit width. $c = \sqrt{g\eta}$, u_i, u_*, n, ν_e, k, ω, ϕ, ρ_a, ρ, c_s, and w_i are the wave speed, velocity, friction velocity, Manning's coefficient of roughness, kinematic viscosity, Karman constant value(=0.41), earth angular velocity($\approx 7.27 \times 10^{-5}$), geographical latitude, atmosphere density, water density, surface friction coefficient, and wind speed. g is the gravitational acceleration. δ and ν_η are the shock-capturing coefficient and artificial viscosity coefficient of the water depth. The boundary conditions are as follows:

$$\boldsymbol{u} = \hat{\boldsymbol{u}} \quad on \quad \Gamma_1 , \tag{2}$$

$$\left(\boldsymbol{\nu}_{ij} \frac{\partial \boldsymbol{u}}{\partial x_j} \right) \cdot \boldsymbol{n} = (\boldsymbol{\nu}_{ij} \boldsymbol{u}_{,j}) \cdot \boldsymbol{n} = \hat{\boldsymbol{t}} \quad on \quad \Gamma_2 , \tag{3}$$

where the Dirichlet and the Neumann boundary conditions are specified on Γ_1 and Γ_2, respectively. In equations (2) and (3), $\hat{\boldsymbol{u}}$ denotes the values given on the boundary, $\boldsymbol{n}$ is the unit outward normal to Γ_2.

3. BUBBLE FUNCTION ELEMENT STABILIZATION METHOD

3.1 Bubble function element

The bubble function element used in the spatial discretization of equation (1) is shown in Figure 2. The bubble function element is expressed as follows:

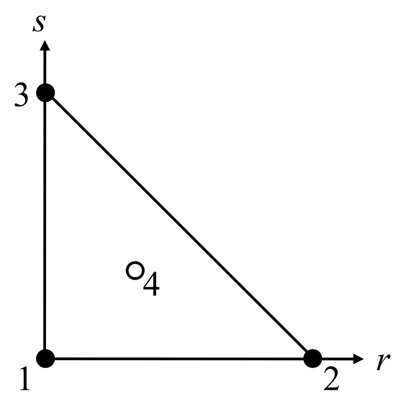

Figure 2: Two-dimensional interpolation function.

$$\boldsymbol{u}_h|_{\Omega_e} = \sum_{\alpha=1}^{3} \Phi_\alpha \boldsymbol{u}_\alpha + \phi_B \boldsymbol{u}_B \ , \ \Phi_\alpha = \Psi_\alpha - \frac{1}{3}\phi_B, \tag{4}$$

$$\Psi_1 = 1 - r - s \ , \ \Psi_2 = r \ , \ \Psi_3 = s. \tag{5}$$

Equation (4) is separated from the linear and bubble function interpolations as follows:

$$\boldsymbol{u}_h|_{\Omega_e} = \bar{\boldsymbol{u}}_h|_{\Omega_e} + \boldsymbol{u}_h^{'}|_{\Omega_e} \ , \ \bar{\boldsymbol{u}}_h|_{\Omega_e} = \sum_{\alpha=1}^{3} \Psi_\alpha \boldsymbol{u}_\alpha \ , \ \boldsymbol{u}_h^{'}|_{\Omega_e} = \phi_B \boldsymbol{u}_B^{'} \ , \ \boldsymbol{u}_B^{'} = \boldsymbol{u}_B - \frac{1}{3}\sum_{\alpha=1}^{3} \boldsymbol{u}_\alpha \ . \tag{6}$$

3.2 Bubble function element stabilization method

The two-level three-level finite element approximation (Matsumoto *et al.*, 2003; Matsumoto, 2005) is considered to be a variation problem of finite element space with the bubble function element. In the two-level three-level finite element approximation, the two-level partition with a two-level bubble function is employed for determination of the finite element solution and the three-level partition with a three-level bubble function is applied to the weighting function. The piecewise linear finite element space $\bar{\boldsymbol{V}}_h$ and the bubble function space $\boldsymbol{V}_h^{'}$, $\hat{\boldsymbol{V}}_h^{'}$ are defined by

$$\bar{\boldsymbol{V}}_h = \{\bar{\boldsymbol{v}}_h \in (H_0^1(\Omega))^3, \ \bar{\boldsymbol{v}}_h|_{\Omega_e} \in (P1(\Omega_e))^3\} \ , \tag{7}$$

$$\boldsymbol{V}_h^{'} = \{\boldsymbol{v}_h^{'} \in (H_0^1(\Omega))^3, \ \boldsymbol{v}_h^{'}|_{\Omega_e} = \phi_B \boldsymbol{v}_B^{'}, \ \boldsymbol{v}_B^{'} \in \mathbf{R}^3\} \ , \tag{8}$$

$$\hat{\boldsymbol{V}}'_h = \{\hat{\boldsymbol{v}}'_h \in (H^1_0(\Omega))^3,\ \hat{\boldsymbol{v}}'_h|_{\Omega_e} = \varphi_B \boldsymbol{v}'_B,\ \boldsymbol{v}'_B \in \mathbf{R}^3\}\ , \tag{9}$$

where ϕ_B and φ_B are the two- and three-level bubble functions with a compact support. In the approximation, the two- and three-level bubble functions are defined elementwise. The approximation is obtained by calculating the finite element solution $\boldsymbol{u}_h \in \boldsymbol{V}_h$, which is determined by the finite element space of $\boldsymbol{V}_h = \bar{\boldsymbol{V}}_h \oplus \boldsymbol{V}'_h$.

$$\langle \dot{\boldsymbol{u}}_h + \boldsymbol{\mathcal{L}}(\bar{\boldsymbol{u}}_{0h})\boldsymbol{u}_h + \boldsymbol{N}(\bar{\boldsymbol{u}}_{0h})\bar{\boldsymbol{u}}_h - \boldsymbol{f}, \hat{\boldsymbol{v}}_h\rangle = 0 \quad \forall \hat{\boldsymbol{v}}_h \in \hat{\boldsymbol{V}}_h\ , \tag{10}$$

where

$$\langle \boldsymbol{u}_h, \boldsymbol{v}_h\rangle := \sum_{e=1}^{N_e} \langle \boldsymbol{u}_h, \boldsymbol{v}_h\rangle_{\Omega_e} := \sum_{e=1}^{N_e} \int_{\Omega_e} \boldsymbol{u}_h \boldsymbol{v}_h\ d\Omega\ ,\ \bar{\boldsymbol{u}}_{0h}|_{\Omega_e} := \frac{1}{A_e}\langle \bar{\boldsymbol{u}}_h, 1\rangle_{\Omega_e}\ ,\ A_e := \int_{\Omega_e} d\Omega.$$

Here, $\langle \cdot, \cdot \rangle_{\Omega_e}$ denotes the L_2-inner product restricted to Ω_e, N_e is the number of elements, and $\bar{\boldsymbol{u}}_{0h}$ is a constant defined elementwise by means of the velocity $\bar{\boldsymbol{u}}_h$ by linear interpolation. The finite element solution $\boldsymbol{u}_h$ that belongs to $\boldsymbol{V}_h$ and the weighting function $\hat{\boldsymbol{v}}_h$ that belongs to

$$\hat{\boldsymbol{V}}_h = \bar{\boldsymbol{V}}_h \oplus \{\boldsymbol{v}'_h + \hat{\boldsymbol{v}}'_h;\ \boldsymbol{v}'_h|_{\Omega_e} + \hat{\boldsymbol{v}}'_h|_{\Omega_e} = (\phi_B + \varphi_B)\boldsymbol{v}'_B\}$$

can be expressed as follows:

$$\boldsymbol{u}_h = \bar{\boldsymbol{u}}_h + \boldsymbol{u}'_h\ ,\ \hat{\boldsymbol{v}}_h = \bar{\boldsymbol{v}}_h + \boldsymbol{v}'_h + \hat{\boldsymbol{v}}'_h = \boldsymbol{v}_h + \hat{\boldsymbol{v}}'_h, \tag{11}$$

where

$$\bar{\boldsymbol{u}}_h,\ \bar{\boldsymbol{v}}_h \in \bar{\boldsymbol{V}}_h\ ,\ \boldsymbol{u}'_h = \sum_{e=1}^{N_e} \phi_B \boldsymbol{u}'_B \in \boldsymbol{V}'_h,$$

$$\boldsymbol{v}'_h = \sum_{e=1}^{N_e} \phi_B \boldsymbol{v}'_B \in \boldsymbol{V}'_h\ ,\ \hat{\boldsymbol{v}}'_h = \sum_{e=1}^{N_e} \varphi_B \boldsymbol{v}'_B \in \hat{\boldsymbol{V}}'_h. \tag{12}$$

The two-level bubble function is used the orthogonal basis bubble function element (Matsumoto, 2005) for P1B element. The orthogonal basis bubble function element has the following relation equation (13).

$$\langle \phi_B, 1\rangle_{\Omega_e} = \langle \phi_B^2, 1\rangle_{\Omega_e} = \frac{N+1}{N+2} A_e. \tag{13}$$

N is space dimension number. It is assumed that the three-level bubble function satisfies the following equations:

$$\langle \Psi_\alpha, \varphi_B\rangle_{\Omega_e} = \frac{1}{N+1}\langle 1, \varphi_B\rangle_{\Omega_e}\ ,\ \alpha = 1 \cdots N+1, \tag{14}$$

$$\langle 1, \varphi_B\rangle_{\Omega_e} = 0\ ,\ \langle \phi_B, \varphi_B\rangle_{\Omega_e} = 0. \tag{15}$$

The finite element that is employed in the bubble function element stabilization method is given as follows:

$$\langle \dot{\boldsymbol{u}}_h, \boldsymbol{v}_h\rangle + \langle \boldsymbol{A}(\bar{\boldsymbol{u}}_{0h})_i \boldsymbol{u}_{h,i}, \boldsymbol{v}_h\rangle + \langle \boldsymbol{\nu}_{ij} \bar{\boldsymbol{u}}_{h,j}, \boldsymbol{v}_{h,i}\rangle + \sum_{e=1}^{N_e} (\boldsymbol{\nu}_{ij} + \boldsymbol{\nu}'_{ij})\langle \phi_{B,j}, \phi_{B,i}\rangle_{\Omega_e} \boldsymbol{u}'_B \boldsymbol{v}'_B$$

$$+\boldsymbol{N}(\bar{\boldsymbol{u}}_{0h})\langle \bar{\boldsymbol{u}}_h, \boldsymbol{v}_h\rangle = \langle \boldsymbol{f}, \boldsymbol{v}_h\rangle + \langle \hat{\boldsymbol{t}} \cdot \boldsymbol{n}, \boldsymbol{v}_h\rangle_{\Gamma_2} \quad \forall \boldsymbol{v}_h \in \boldsymbol{V}_h\ . \tag{16}$$

Here, ν_η is set to zero. The stabilized operator control term $(\boldsymbol{\nu}_{ij}+\boldsymbol{\nu}'_{ij})\langle\phi_{B,j},\phi_{B,i}\rangle_{\Omega_e}\boldsymbol{u}'_B$ is derived from the three-level bubble function. $\boldsymbol{\nu}'_{ij}$ is expressed as follows,

$$\boldsymbol{\nu}'_{11}=\begin{bmatrix}\nu'_\eta & 0 & 0\\ -2u_1\nu'_1 & 2\nu'_1 & 0\\ -u_2\nu'_2 & 0 & \nu'_2\end{bmatrix}\ ,\ \boldsymbol{\nu}'_{12}=\begin{bmatrix}0 & 0 & 0\\ 0 & 0 & 0\\ -u_1\nu'_2 & \nu'_2 & 0\end{bmatrix}\ ,$$

$$\boldsymbol{\nu}'_{21}=\begin{bmatrix}0 & 0 & 0\\ -u_2\nu'_1 & 0 & \nu'_1\\ 0 & 0 & 0\end{bmatrix}\ ,\ \boldsymbol{\nu}'_{22}=\begin{bmatrix}\nu'_\eta & 0 & 0\\ -u_1\nu'_1 & \nu'_1 & 0\\ -2u_2\nu'_2 & 0 & 2\nu'_2\end{bmatrix}.$$

The stabilized operator control parameter $\boldsymbol{\nu}'_{ij}$ can be determined as follows (Matsumoto *et al.*, 2003; Matsumoto, 2005) :

$$(\boldsymbol{\nu}_{ij}+\boldsymbol{\nu}'_{ij})\langle\phi_{B,j},\phi_{B,i}\rangle_{\Omega_e}\boldsymbol{u}'_B=\frac{\langle\phi_B,1\rangle^2_{\Omega_e}}{A_e}\boldsymbol{\tau}^{-1}_{eR}\boldsymbol{u}'_B\ , \tag{17}$$

where

$$\boldsymbol{\tau}_{eR}=\begin{bmatrix}\tau_{e\eta} & 0 & 0\\ 0 & \tau_{eu} & 0\\ 0 & 0 & \tau_{eu}\end{bmatrix}\ ,\ \tau_{e\eta}=\frac{1}{|\tau_{SUGN1}|}\ ,\ \tau_{eu}=\left\{\frac{1}{(\tau_{SUGN1})^2}+\frac{1}{(\tau_{SUGN2})^2}\right\}^{-\frac{1}{2}}\ ,$$

$$\tau^{-1}_{SUPG1}=\left\{\sum_{\alpha=1}^{3}\left(c|\boldsymbol{j}\cdot\nabla\Psi_\alpha|+|\boldsymbol{u}^h\cdot\nabla\Psi_\alpha|\right)\right\}\ ,\ \boldsymbol{j}=\frac{\nabla\eta}{\|\nabla\eta\|}\ ,\ \boldsymbol{u}^h=[u\ v]^T\ ,$$

$$\tau^{-1}_{SUPG2}=4\nu_e h^{-2}_{RGN}\ ,\ h^{-1}_{RGN}=2\left(\sum_{\alpha=1}^{3}|\boldsymbol{r}\cdot\nabla\Psi_\alpha|\right)\ ,\ \boldsymbol{r}=\frac{\nabla\|\boldsymbol{u}^h\|}{\|\nabla\|\boldsymbol{u}^h\|\|}\ .$$

h_{RGN} is the element length (Tezduyar and Senga, 2006).

4. TEMPORAL DISCRETIZATION

4.1 Jameson-Baker's m-step Runge-Kutta method

Finally, the finite element equation (16) can be expressed as follows:

$$\boldsymbol{M}\dot{\boldsymbol{u}}_h+\boldsymbol{F}(\boldsymbol{u}_h)=0. \tag{18}$$

In the temporal discretization, an explicit method is employed in this study. For the finite element equation (18), the time discretization based on Jameson-Baker's m-step Runge-Kutta method (Jameson and Baker, 1983) is given by

$$l=0,1,\ldots,m-1\ \ ,\ \ \boldsymbol{u}_h^{n+1/(m+1)}=\boldsymbol{u}_h^n,$$

$$\boldsymbol{M}\boldsymbol{u}_h^{n+1/(m-l)}=\boldsymbol{M}\boldsymbol{u}_h^n-\frac{\Delta t}{m-l}\boldsymbol{F}(\boldsymbol{u}_h^{n+1/(m+1-l)}). \tag{19}$$

Δt and n denote the time increment and time step.

4.2 Mass matrix of bubble function element

The mass matrix of the bubble function element will be described in this section. The mass matrix of each element in the two-dimensional bubble function element is expressed as follows:

$$\langle \boldsymbol{\Phi}, \boldsymbol{\Phi}^T \rangle_{\Omega_e} = \boldsymbol{M}_{mn}^{(e)} = \begin{bmatrix} \frac{A_e}{6} & \frac{A_e}{12} & \frac{A_e}{12} & 0 \\ \frac{A_e}{12} & \frac{A_e}{6} & \frac{A_e}{12} & 0 \\ \frac{A_e}{12} & \frac{A_e}{12} & \frac{A_e}{6} & 0 \\ 0 & 0 & 0 & 0 \end{bmatrix}$$

$$+\frac{1}{9}\langle \phi_B, 1 \rangle_{\Omega_e} \begin{bmatrix} -2 & -2 & -2 & 3 \\ -2 & -2 & -2 & 3 \\ -2 & -2 & -2 & 3 \\ 3 & 3 & 3 & 0 \end{bmatrix} + \frac{1}{9}\langle \phi_B, \phi_B \rangle_{\Omega_e} \begin{bmatrix} 1 & 1 & 1 & -3 \\ 1 & 1 & 1 & -3 \\ 1 & 1 & 1 & -3 \\ -3 & -3 & -3 & 9 \end{bmatrix}, \tag{20}$$

$$m = 1, \cdots, 4 \ , \ n = 1, \cdots, 4 \ ,$$

$$\boldsymbol{\Phi} = [\Phi_1 \ \Phi_2 \ \Phi_3 \ \phi_B]^T.$$

Here, ϕ_B is an arbitrary two-level bubble function that conforms to the bubble function. The mass matrix of the bubble function element is determined on the basis of the following two integration values.

$$\langle \phi_B, 1 \rangle_{\Omega_e} \ , \ \langle \phi_B, \phi_B \rangle_{\Omega_e}. \tag{21}$$

The following integration values are used in the case of a linear bubble function (Matsumoto, 2006).

$$\langle \phi_B, 1 \rangle_{\Omega_e} = \frac{1}{3}A_e \ , \ \langle \phi_B, \phi_B \rangle_{\Omega_e} = \frac{1}{6}A_e. \tag{22}$$

A consistent mass matrix of the bubble function element is obtained as follows:

$$\boldsymbol{M}_{mn}^{(e)} = \frac{A_e}{36} \begin{bmatrix} 4 & 1 & 1 & 2 \\ 1 & 4 & 1 & 2 \\ 1 & 1 & 4 & 2 \\ 2 & 2 & 2 & 6 \end{bmatrix}. \tag{23}$$

The mass matrix of the linear bubble function element is not a diagonal matrix. Therefore, the lumping of the mass matrix is required to solve the m-step Runge-Kutta method efficiently. The lumped mass matrix of the linear bubble function element is given by

$$\boldsymbol{M}_{mn}^{(e)} \approx \text{diag}\left(\sum_{n=1}^{4} \boldsymbol{M}_{mn}^{(e)} \right) = \frac{A_e}{9} \begin{bmatrix} 2 & & & \\ & 2 & & \\ & & 2 & \\ & & & 3 \end{bmatrix}. \tag{24}$$

On the other hand, following are the integration values for the case of an orthogonal basis bubble function (Matsumoto, 2005).

$$\langle \phi_B, 1 \rangle_{\Omega_e} = \langle \phi_B, \phi_B \rangle_{\Omega_e} = \frac{N+1}{N+2}A_e \ , \ N = 2. \tag{25}$$

By substituting equation (25) into equation (20), the consistent mass matrix of the bubble unction element is obtained as follows:

$$\boldsymbol{M}_{mn}^{(e)} = \frac{A_e}{12} \begin{bmatrix} 1 & & & \\ & 1 & & \\ & & 1 & \\ & & & 9 \end{bmatrix}. \tag{26}$$

An important point to be noted is that the consistent mass matrix $\boldsymbol{M}$ is a diagonal matrix on account of the orthogonal intersection of the basis functions of the orthogonal basis bubble function element.

5. WIND-DRIVEN CURRENT PROBLEM

The wind-driven current problem (Csanady, 1982) is used to investigate the numerical accuracy of the bubble function element stabilization method as a numerical example. Figure 3 shows the computational model and mesh type. This problem has the following exact solution.

$$\zeta = \frac{c_s}{\rho g h} x - \frac{4\ l\ c_s}{\pi^2 \rho g h} \left\{ \sum_{n=1}^{\infty} \frac{(-1)^{n+1}}{(2n-1)^2}\ \cos \frac{(2n-1)\pi c t}{l}\ \sin \frac{(2n-1)\pi x}{l} \right\} \tag{27}$$

In the finite element mesh, 200 × 4 divisions are performed. The total numbers of nodes and elements are 1007 and 1604, respectively. The numerical results obtained after 50.0

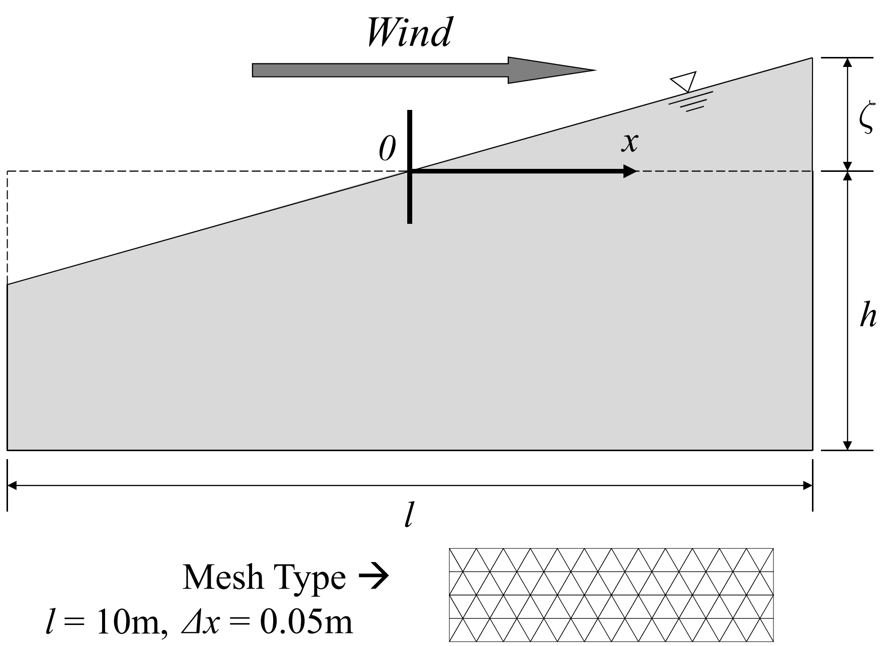

Figure 3: Computational model and mesh type.

s are shown in Figure 4. Figure 4 is the results of the point of x=0.25 with the central points to y axis. The numerical results are used Δt=0.001 s and m=4. The numerical results shown in Figure 4 indicate the results with the stabilized operator control term. "Lumped mass matrix" indicates the result of a linear bubble function element. "Diagonal mass matrix" indicates the result of an orthogonal basis bubble function element. The result of the diagonal mass matrix is in a better agreement with the exact solution than the result of the lumped mass matrix, as shown in Figure 4.

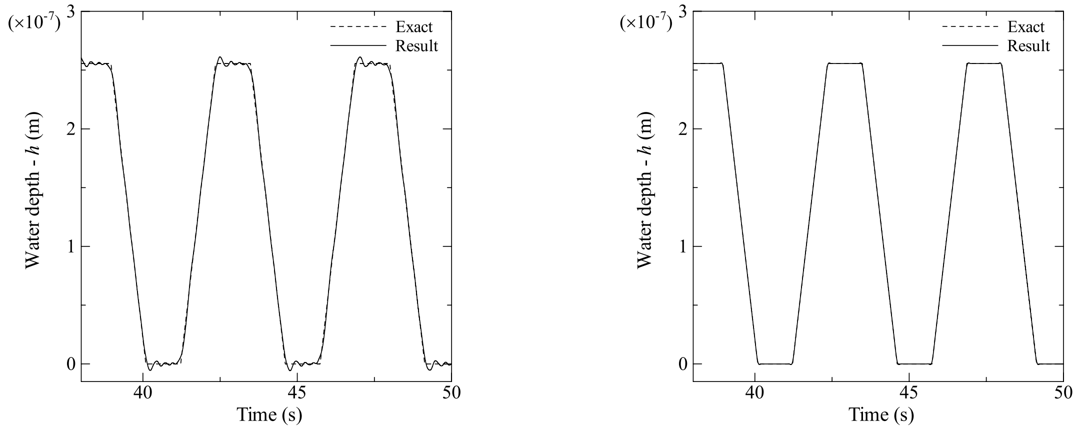

(a) Lumped mass matrix (b) Diagonal mass matrix

Figure 4: Numerical results of after 50.0 s.
($n = 0$, $c_s = 0.001$, $h = 2m/s$, $\rho = 998.2kg/m^3$, $\rho_a = 1kg/m^3$, $w_1 = 1m/s$, $w_2 = 0$, $\delta = 0$)

6. DAM-BREAK PROBLEM

6.1 Numerical example 1

In order to investigate the numerical accuracy and stability of stabilized bubble function method, dam-break problem (Stoker, 1957) is used numerical example. Figure 5 shows the computational model and mesh type. The numerical results at 1.0 s of water depth

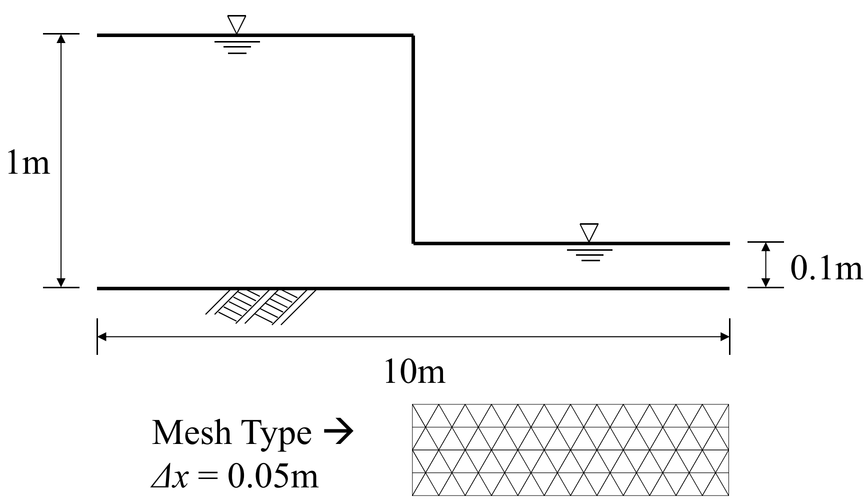

Figure 5: Computational model and mesh type.

and velocity are shown in Figures 6-7. The results of these figures are the values on y axis. The domain is divided into 200 equal-length elements. The numerical results are used Δt=0.001 s and m=4. We compare the results of water depth and velocity by using classical bubble function element and bubble function element stabilization method. The classical bubble function element means the bubble function element without the stabilized operator control term in equation (16). The spatial oscillation of water depth and velocity is very serious in the result from classical bubble function element. However, the bubble function element stabilization method remedies the oscillation distribution of water depth and velocity.

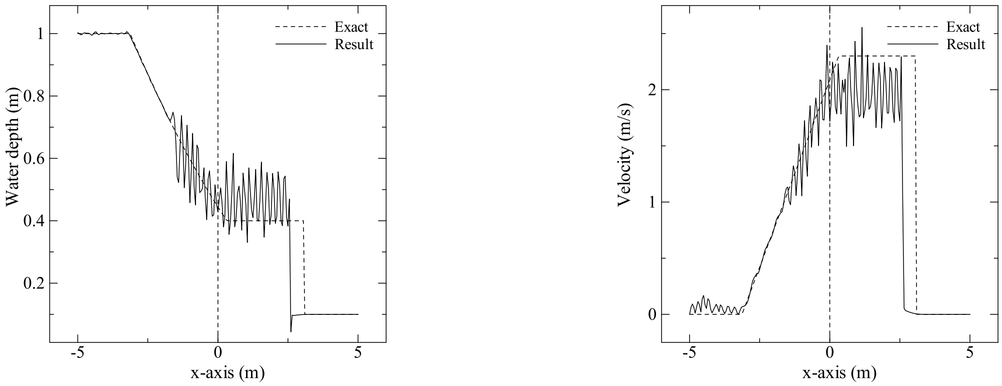

Figure 6: Classical bubble function element. ($n = 0$, $c_s = 0$, $\delta = 0$)

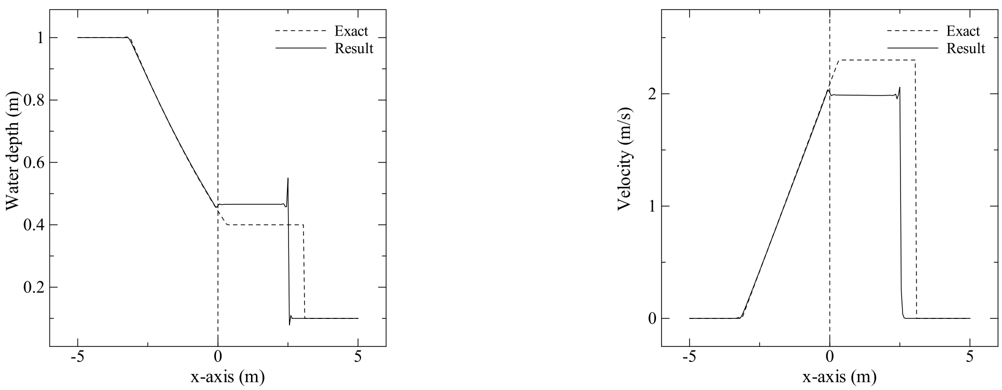

Figure 7: Bubble function element stabilization method. ($n = 0$, $c_s = 0$, $\delta = 0$)

6.2 Numerical example 2

In numerical example 1, the results for bubble function element stabilization method oscillate the discontinuous parts. Therefore, shock-capturing term requires this problem. In this study, a shock-capturing coefficient based on the reference (Tezduyar and Senga, 2006) is proposed as follows

$$\delta = \frac{h_{RGN}}{2} \lambda \left(\frac{\langle u_k^{h'}, u_k^{h'} \rangle_{\Omega_e}}{\langle \bar{u}_k^h, \bar{u}_k^h \rangle_{\Omega_e}} \right)^{r_e} \ , \ \lambda = \frac{h_{RGN}}{2} (\tau_{SUGN1})^{-1} \ , \ r_e = 0.15 \ . \qquad (28)$$

Figure 8 is numerical results at 1.0 s with shock-capturing term using bubble function element stabilization method. The results of bubble function element stabilization method are in good agreement with the results of exact solutions.

7. CONCLUSION

In this paper, the bubble function method stabilization method for shallow water long wave equation was investigated. The result of the diagonal mass matrix is in a better agreement with the exact solution of the wind-driven current problem than the result of the lumped mass matrix. The bubble function method stabilization method obtained better numerical accuracy and stability than the classical bubble function method with Bubnov-Galerkin formulation.

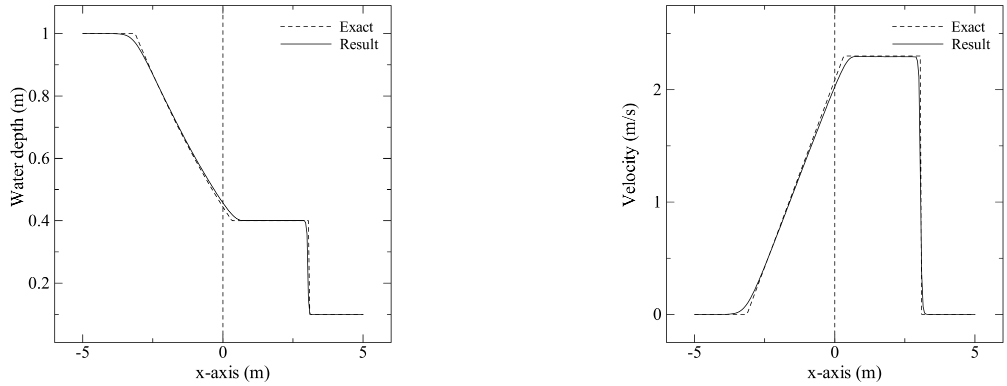

Figure 8: Bubble function element stabilization method + shock capturing term. ($n = 0$, $c_s = 0$)

REFERENCES

Pierre, R. (1988), Simple C^0 approximations for the computation of incompressible flows, *Comput. Methods Appl. Mech. Engrg.*, 68, pp.205-227.

Baicocchi, C., Brezzi, F., and Franca, L.P. (1993), Virtual bubbles and Galerkin-least-squares type method(Ga.L.S.), *Comput. Methods Appl. Mech. Engrg.*, 105, pp.125-141.

Brooks, A.N. and Hughes, T.J.R. (1982), Streamline upwind / Petrov-Galerkin formulations for convection dominated flows with Navier-Stokes equations, *Comput. Methods Appl. Mech. Engrg.*, 32, pp.199-259.

Simo, J.C., Armero, F., and Taylor, C.A. (1995), Stable and time-dissipative finite element methods for the incompressible Navier-Stokes equations in advection dominated flows, *Int. J. Numer. Meth. Engng.*, 38, pp.1475-1506.

Yamada, T. (1998), A bubble element for the compressible Euler equations, *Int. J. Comput. Fluid Dyn.*, 9, pp.273-283.

Matsumoto, J., Umetsu, T., and Kawahara, M. (2003), Stabilized bubble function method for shallow water long wave equation, *Int. J. Comput. Fluid Dyn.*, 17(4), pp.319-325.

Matsumoto, J. (2005), A relationship between stabilized FEM and bubble function element stabilization method with orthogonal basis for incompressible flows, *J. Appl. Mech., JSCE*, 8, pp.233-242.

Jameson, A. and Baker, T.J. (1983), Soluiton of the Euler equations for complex configurations, *AIAA Paper*, pp.83-1929.

Matsumoto, J. (2006), A Fractional Step Method for Incompressible Viscous Flow Based on Bubble Function Element Stabilization Method, *Int. J. Comput. Fluid Dyn.*, 20(3-4), pp.145-155.

Csanady, G. T. (1982), Circulation in the coastal ocean, *D. Reidel. Pub.*

Stoker, J.J. (1957), Water waves (The mathematical theory with applications), *Interscience Publishers, New York.*

Tezduyar, T.E. and Senga, M. (2006), Stabilization and shock-capturing parameters in SUPG formulation of compressible flows, *Comput. Methods Appl. Mech. Engng.*, 195, pp.1621-1632.

TECHNICAL CONTRIBUTIONS

CFD Computational Methods